

## EXPERIMENTAL DETERMINATIONS OF THE COHERENT SCATTERING DOMAIN SIZE DISTRIBUTION OF NATURAL MICA-LIKE PHASES WITH THE WARREN-AVERBACH TECHNIQUE

**Key Words**—Crystallite size, Fit, Fourier analysis, Illite, Illite/smectite, Peak broadening, Warren-Averbach, X-ray powder diffraction.

### INTRODUCTION

X-ray diffraction (XRD) has recently undergone a complete transformation with the availability of computer-driven diffractometers. The resulting digitized data, combined with increasingly powerful computers, allow numerous calculation routines for numerical data processing to get more information out of an XRD profile. A decomposition routine, for example, enables the separation of the respective contributions of phases with distinct but closely related crystallographic characteristics from a complex XRD profile (Lanson and Champion, 1991; Righi and Meunier, 1991). In addition, quoting Klug and Alexander (1974), "Appropriate analysis of the line profile should yield such information as . . . the mean size of coherent crystalline domain, distribution of crystallite sizes, and the nature and extent of lattice imperfections." Kodama *et al.* (1971) developed a Fourier analysis of XRD profiles to establish the mean coherent scattering domain size (CSDS) of microcrystalline muscovites, as well as the variation of their interlayer spacings. More recently the Warren-Averbach (WA) technique (Warren and Averbach, 1950) has been used to determine the CSDS distribution (Eberl and Srodon, 1988; Eberl *et al.*, 1990) of sericite- and illite-rich samples. Information on CSDS is especially important when looking at mineral transformation and/or growth.

This paper has been inspired by some unusual results and correlations obtained by using the WA technique to determine CSDS distributions on various samples containing mostly illitic phases. It does not answer any of the questions it asks, but is intended to be a warning signal to some of the limitations of the newly available calculation routines. The increasing number of algorithms, often presented as "black-box" packages, made us wonder about the reliability and the limitations of these programs. These routines are obviously very useful and provide a significant amount of information, but could be even more relevant if the user is aware of the theoretical limitations of these programs. It would also be useful for the user to know if any simplifying hypotheses, including the convergence criteria for the

fitting routines (e.g.), have been used while developing the algorithm and what their possible effects are.

The purpose of this note is not to provide a detailed description of the various methods that may be used to determine crystallite size, as well as lattice distortions, through X-ray diffraction line profile analysis. The interested reader may refer to Klug and Alexander (1974), Kodama *et al.* (1971), Delhez *et al.* (1982), and Keijser *et al.* (1982), for a comprehensive description of these methods. However, a basic knowledge of line-broadening Fourier analysis is necessary to understand the limitations resulting from the different steps of data processing. The presentation below follows essentially the description of Louër (1986).

An X-ray diffraction pattern (also denoted as *h* profile) contains three components that are convoluted: the diffraction profile of the specimen (also denoted as *f* profile), which is of interest; the geometrical aberrations of the instrument; and the emission profile of the radiation. The convolution of the latter two (also denoted as *g* profile) is determined experimentally by using a standard specimen with the same chemical composition as the unknown, and negligible diffraction broadening. A deconvolution procedure is applied to obtain the line profile *f*, which is expressed then as a Fourier series. The Fourier cosine coefficients,  $A_n$ , are the product of a size coefficient,  $A_n^s$ , and of a distortion coefficient,  $A_n^d(l)$ , with *l* being the order of reflection. A method for separating the two components was proposed by Warren and Averbach (1952). The mean apparent size is obtained from the initial slope of the curve  $A_n^s$  versus *L* [where  $L = n/\Delta_s$ , *n* being the harmonic number,  $\Delta_s = 2\sin \theta_2/\lambda - 2\sin \theta_1/\lambda$ , when  $(\theta_1, \theta_2)$  is the angular range over which the profiles are measured, and  $\lambda$  is the wavelength of the radiation]. In strain-free materials, the distribution  $P(n)$  of column of length *n* unit cells can be evaluated from the second derivative of  $A_n^s$  with respect to *n* (Bertaut, 1950) or directly from *f* (Louër, 1986).

### EXPERIMENTAL METHODS

Unrelated examples from extremely varied locations and origins were chosen to evaluate the WA method.

Forty-three samples of drill cuttings were selected from a deep borehole in the Eastern Paris Basin. These samples are Stephanian to Permian in age, and have been extensively described by Lanson and Champion (1991) and Lanson and Velde (1992). An additional ten samples came from the Upper Cretaceous Niger Delta mudstones described by Velde *et al.* (1986). Four more samples were from the Glarus thrust (Swiss Alps) described by Burkhard *et al.* (1992), and four others from the Helvetic nappes of Western Switzerland. The latter samples are Malm in age (S. Huon, personal communication). An illite-rich sample was supplied by D. K. McCarty from a surface outcrop of the middle Devonian Tioga bentonite in the Onondaga limestone Formation (central New York State). All these samples contain mostly micaceous clays. However, some samples (e.g., from Paris basin) contain a slightly expandable (<10% smectite) illite/smectite mixed-layer coexisting with purely illitic clays (Lanson and Velde, 1992). The different size fractions (usually the <2.0  $\mu\text{m}$  fraction) were obtained by centrifugation or sedimentation, and oriented slides were prepared according to the procedures described by the various authors listed above.

The oriented glass slides were all step-scanned on a Siemens D500 XRD system using  $\text{CuK}\alpha(1 + 2)$  radiation, a graphite monochromator,  $1^\circ$  divergence and receiving slits, soller slits on the diffracted beam, and the Siemens D5000 software (version 2.3) running on a Microvax 2000. The WA analysis was performed using the 002 and 005 XRD reflections as suggested by Eberl and Srodon (1988). XRD patterns were collected from  $14$  to  $24^\circ 2\theta$  ( $6.3$  to  $3.7 \text{ \AA}$ ) and from  $42$  to  $50^\circ 2\theta$  ( $2.15$  to  $1.80 \text{ \AA}$ ), counting respectively 6 and 6 to 10 seconds per  $0.02^\circ 2\theta$  step. Prior to the Fourier analysis, the fit procedure was performed with a split-Pearson function using separate exponents; the use of this asymmetrical profile makes it possible to fit either reflection with a unique set of parameters. XRD profiles were fitted usually from  $16.0$  to  $19.5^\circ 2\theta$  ( $5.5$  to  $4.5 \text{ \AA}$ ) and from  $43.0$  to  $47.5^\circ 2\theta$  ( $2.10$  to  $1.90 \text{ \AA}$ ). The results were considered adequate when the R value, that is  $(|\text{Exp} - \text{Calc}|)/(|\text{Exp}|)$  where Exp and Calc represent respectively the experimental and fitted profiles, is lower than 0.05; most often, R values were about 0.02. The WA analysis was performed then, using as starting values the results of the fit procedures carried out on the 002 and 005 peaks of both the sample of interest and of the reference. The ground muscovite standard pattern used to determine the broadening of the pure diffraction line profile induced by instrumental factors is the one collected by Eberl and Srodon (1988). The Fourier analysis was performed mostly on the profiles obtained from air-dried samples, as suggested by Eberl and Blum (1993). The patterns of eight ethylene-glycol solvated samples from Switzerland were

also analysed. Basically, the results are consistent with the air-dried samples, and are not discussed separately.

To determine the CSDS one can use also the Scherrer equation (Klug and Alexander, 1974):  $L = K\lambda/(B \cos \theta)$ , where L is the mean crystallite thickness, in  $\text{Å}$ , along  $c^*$  axis, K is a constant equal to 0.91 (Brindley, 1980),  $\theta$  is the diffraction angle, and B is the peak breadth at half maximum intensity measured in radians. In this study, experimental peak breadths have not been corrected for instrumental broadening; consequently, mean CSDS may have been slightly underestimated.

## RESULTS AND DISCUSSION

### *Experimental results*

The Paris Basin samples (Figure 1) have been characterized thoroughly by image analysis of transmission electron micrographs, X-ray fluorescence chemical analysis (Lanson and Champion, 1991) and decomposition of XRD profiles (Lanson and Velde, 1992). The simultaneous occurrence of three "illitic" phases (i.e., highly illitic illite/smectite mixed-layer or I/S, poorly crystallized illite and well crystallized illite) has been shown on the various diffraction peaks (001, 002, 003 and 005 bands) of the  $2$ – $50^\circ 2\theta$  ( $44$  to  $1.8 \text{ \AA}$ ) range (Lanson and Velde, 1992). Because of the relative intensity (Table 1) of the well crystallized (CSDS > 20 layers) illite peak, one could expect the presence of some high CSDS values (above 20 nm) in the distribution determined with the WA technique. Conversely, the WA analysis of sample C1730 indicates that 99.1% of the particles are less than ten layers thick. The total absence of these high values (Figure 2) is quite surprising. Further, the mean CSDS of sample C1730 has been determined by using Scherrer equation (Table 2). Except for the 8.1 nm value estimated from the 001 peak which is affected by interstratification broadening, the mean CSDS values obtained from 002, 003 and 005 peaks are very consistent around 11.5 nm. These values are consistent with the mean CSDS of about 12–15 layers deduced from the intensity ratio ( $I_r = 1.87$ ) versus Kubler index ( $KI = 1.03^\circ 2\theta \text{ Cu}$ ) plot of Eberl and Velde (1989). This plot also confirms the highly illitic nature of sample C1730, indicating 7% of expandable layers, in agreement with the results from XRD profile decomposition (Lanson and Velde, 1992). Conversely, the WA analysis of sample C1730 (Figure 2, Table 3) indicates a mean CSDS of 1.6 nm that is totally inconsistent with other mean particle thickness data.

In summary, the total absence of large CSDS values (above 15 nm) is inconsistent with the presence of well crystallized illite demonstrated by Lanson and Velde (1992). Further, the CSDS distributions obtained with the WA technique for the Paris Basin samples are inconsistent with previously available data. The very low

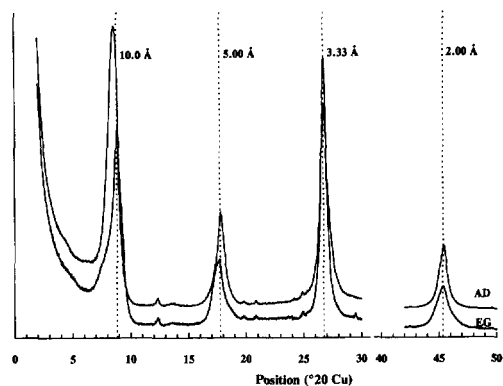


Figure 1. X-ray diffraction pattern of sample C1730, from the Paris Basin borehole C.

mean CSDS values (from 1.0 to 3.0 nm, i.e., 1 to 3 layers on average, for 29 out of the 43 samples) seem unrealistic for such highly illitic samples (the I/S, associated with pure illite, contains less than 10% smectite) and are contradictory with the values derived from Scherrer equation and from the diagram of Eberl and Velde (1989). XRD diagrams of highly illitic I/S (94% illite) were simulated with CALC (Lanson and Besson, 1992) assuming an average CSDS of twelve layers on the one hand and using the CSDS distribution obtained from WA analysis on the other hand (Figure 3). The latter profile is influenced mostly by the structure factor of illite and is very different from the experimental pattern, whereas the profile calculated using a twelve layer mean CSDS agrees reasonably well with the experimental pattern and supports the validity of this CSDS data. Such unrealistic very low mean CSDS values, that are less than three layers on average, have been determined not only for 29 samples out of the 43 from the Paris Basin but for all samples from Niger Delta mudstones, and for the various size fractions of the Devonian bentonite as well.

Additionally, when plotting the width at half maximum of the CSDS frequency distribution versus the mean CSDS (Figure 4) one can observe a very good

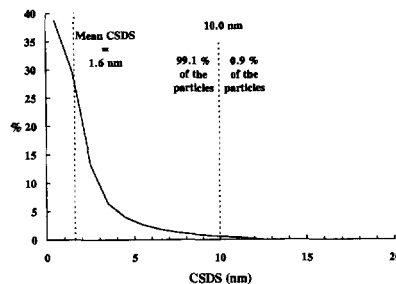


Figure 2. Example of coherent scattering domain size frequency distribution determined with the Warren-Averbach technique on sample C1730, from the Paris Basin borehole C. The algorithm was performed using a split-Pearson (separate exponents) function to fit both the 002 and the 005 XRD peaks of the air-dried sample.

correlation ( $r^2 = 0.990$ ) between these two parameters. At first, there seems to be no reason for both parameters to be so closely related. However, one can think of various hypotheses to explain such a correlation: 1) chance in the sample selection; 2) this relation is induced by the calculation algorithm; 3) the CSDS distributions are similar (lognormal tendency) because the formation and growth mechanisms are the same for all these micaceous phases, as suggested by Eberl *et al.* (1990); or 4) the WA technique could not be applied to our samples because of their nature, or the method was not applied the right way. The first three hypotheses will not be discussed because we lack any information about them.

#### Fourier analysis of X-ray diffraction profile broadening

Prior to addressing the fourth hypothesis, one should be convinced that the Fourier analysis of X-ray diffraction profile broadening itself, which has been widely used in the last four decades, especially in the field of metals, and whose results have been checked successfully against other measurements, is not questionable. For example, Kodama *et al.* (1971) developed an original Fourier analysis of XRD profile broadening to

Table 1. Illite content, mean coherent scattering domain size (CSDS), and relative intensities of the phases producing the three elementary peaks fitted to the various peaks of sample C1730.

	Well crystallized illite			Poorly crystallized illite			Illite/smectite mixed-layer		
	Illite content	Mean CSDS	Relative intensity	Illite content	Mean CSDS	Relative intensity	Illite content	Mean CSDS	Relative intensity
001	96%	22–25	25%	100%	6–9	41%	NA	NA	34%
002	NA	NA	28%	NA	NA	36%	NA	NA	36%
003	97%	22–25	39%	99%	6–9	42%	91%	6–9	19%
005	96%	22–25	39%	100%	6–9	39%	92%	4–7	22%

Illite content and mean CSDS as determined by Lanson and Velde (1992) by comparison with calculated patterns. NA: identification data not available because of the mismatch between experimental and simulated position-full width at half maximum intensity values.

Table 2. Mean crystallite thickness determined by applying the Scherrer equation to the various peaks of sample C1730.

Peak	Mean crystallite thickness
001	8.1 nm
002	11.5 nm
003	11.4 nm
005	11.4 nm

estimate at first the mean deviation from the ideal d-spacing (i.e., strain), and as a second step the mean CSDS for microcrystalline muscovites. Their results correlate well with the total number of interlayer cations.

The standard WA approach has been used on binary alloys or metallic oxides by various authors (Wagner and Aqua, 1963; Roof, 1971; Baggerly, 1974; Huang and Parrish, 1978) to determine either the mean CSDS, the strain in the lattice, or the CSDS distribution. The measurements may be performed along any crystallographic direction, and usually are checked against other XRD measurements (integral breadth or variance methods) or by direct transmission electron microscope (TEM) observations. Louër (1986) used the WA technique to follow strain-free zinc oxide crystallite growth along several *hkl* directions and consequently to characterize a change in the morphology of the crystallites from a cylinder to a hexagonal prism. He demonstrated that the apparent sizes obtained using the variance method agree with the ones determined from the WA analysis, and that crystallite shape observed with TEM confirms the model proposed from XRD profile analysis.

However the initial question of why the WA technique gives an answer inconsistent with previously available data for our samples remains unanswered. The successive steps of the procedure are examined and the various implied limitations are checked in order to point out the possible restrictions to the use of the WA analysis for clay minerals on the one hand, and the special care that should be taken to perform a correct analysis on the other hand.

**Determination of the instrumental profile.** The *g* profile, which results from the convolution of the geometrical aberrations of the instrument and of the emission profile of the radiation, is determined experimentally by running a standard specimen with the same chemical composition as the sample. According to Klug and

Table 3. Mean crystallite thickness and mode of the CSDS frequency distribution determined by performing the WA procedure (see text for details) on sample C1730.

Mean crystallite thickness	1.6 nm
Mode of CSDS distribution	0.9 nm

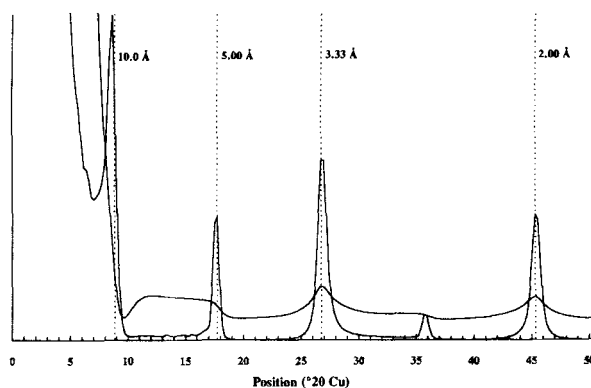


Figure 3. X-ray diffraction patterns calculated with CALC (Lanson and Besson, 1992). Both profiles were simulated assuming a 94% illite mixed-layer illite/smectite with maximum ordering ( $R = 1$ ). The upper profile has been calculated with the CSDS distribution obtained from the WA analysis of sample C1730. The lower profile has been calculated assuming a triangular distribution of CSDS from 7 to 17 layers (mean CSDS = 12 layers).

Alexander (1974) the chosen reference powder should “produce diffraction lines in the immediate neighborhood of the lines of the unknown to be measured.” Obviously by using a mica standard, this requirement is fulfilled. Additionally, these authors point out that the reference should be “a substance not subject to lattice distortions, which would produce line broadening.” Indeed, as pointed out by Louër and Langford (1988), “a common source of systematic error in line-profile analysis is the use of an ‘instrumental’ standard which itself exhibits sample broadening.” Kodama *et al.* (1971) show that for microcrystalline muscovites

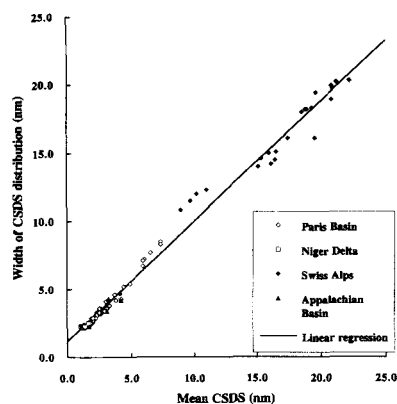


Figure 4. Full width at half maximum of the coherent scattering domain size distribution versus the mean coherent scattering domain size as determined by the Warren-Averbach technique. There are more data points than listed samples because some samples were run on both air-dried and ethylene glycol-solvated states and because various size fractions were run for some other samples. Linear regression coefficient of determination  $r^2 = 0.990$ .

the d-spacings may vary by up to 0.036 Å about the ideal d-value, if the distribution of interlayer cations is irregular. Consequently, the mica standard should be selected very carefully to prevent the presence of strain-broadening. It would be interesting also to investigate both feasibility and influence of a thermal processing similar to annealing of alloys for the reference powder.

*Determination of the background.* Klug and Alexander (1974) point out that most often the determination of the pure line profile, which is an essential step to the calculation of the crystallite size, is not satisfactory because of noise in the experimental data and/or of misplacement of the background. With modern diffractometers, experimental noise is not a major problem any more if counting times sufficient to obtain a good statistics (i.e., at least  $10^4$  counts at peak maximum) are used. However, the determination of background remains a difficulty in line profile analysis, especially for very broad peaks. Inaccuracies in background determination translate usually in Fourier space into a "hook" effect, that is a negative curvature of the  $A_n^S$  curve near  $n = 0$ , but may lead to large errors in the structural parameters obtained from line profile analysis (Delhez *et al.*, 1982).

*Presence of strains.* Klug and Alexander (1974) also state that "an estimate of the size distribution," may be obtained only "in favorable circumstances," that is, in the absence of strains inducing lattice distortions. This condition, which is unlikely to be matched even for purely non-expandable material, severely impairs the application of the method to clay minerals. Kodama *et al.* (1971) measured variations (i.e., strains) up to 0.036 Å about the ideal d-spacing on microcrystalline muscovites. Both the assumptions of a constant strain broadening associated with interparticle swelling at 17 Å (Eberl and Srodon, 1988) and of the absence of broadening induced by mixed-layering for even-order reflections of Ca-saturated (2 water-layer smectite) illitic I/S (Eberl and Blum, 1993) also seem unrealistic. Srodon (1980) and Sato *et al.* (1992) indeed showed that the basal spacing of a homoionic smectite (hydrated or ethylene-glycol solvated) varies significantly as a function of layer charge, charge location, relative humidity, and expansion energy.

*Small crystallite size.* Klug and Alexander (1974) indicate that the approximation of  $\sin^2(\pi h_3)$  by  $(\pi h_3)^2$  made by Warren and Averbach (1950) is less accurate for small crystallite sizes (Bienenstock, 1961), which is undoubtedly the case for clay minerals. For very broad diffraction lines, induced by fine-grained materials, it may be necessary also to take into account the variation of the structure factor within the considered angular range. Siemens (1990) actually warns the user

of its WA program that average crystallite sizes smaller than 5 nm may lack any physical meaning.

Finally, the WA method was run on our samples taking only two reflections into account, but Klug and Alexander (1974) argue that an extrapolation from three or more orders is preferred. For the reasons detailed above, it seems that the use of the WA technique on clays is inappropriate. However, one should note that the results obtained with this technique by Eberl and Srodon (1988), using the same instrumental standard and a procedure very similar to the one used for this study, correlate well with their TEM thickness measurements.

## SUMMARY AND CONCLUSIONS

Our results show that there is a large difference (inconsistency) between the grain-size estimations determined by using a decomposition and simulation approach, Scherrer equation or the diagram proposed by Eberl and Velde (1989) on the one hand or the WA technique on the other hand. These differences are probably due to initial conditions required to apply the WA procedure that are not met by our samples (e.g., presence of strains, very fine-grained minerals). One should note that the above results have been obtained using the WA calculation procedure as a routine without any special care, and their inconsistency with previously available data is possibly induced by an improper use of the method. However, because these conditions may be used commonly it seemed interesting to point out that assumptions made to use the WA method on clay-size micas and micaceous phases may be unwarranted. Consequently, one must be aware that the effects of neglected parameters may not be small enough to justify the approximations.

Despite these limitations the WA technique remains a very interesting technique: it is easy and fast to perform, and provides statistical information that can be obtained otherwise only with transmission electron microscopy (high resolution or Pt-shadowing) and a huge amount of time-consuming particle thickness measurements.

## ACKNOWLEDGMENTS

We thank the Institut Français du Pétrole, M. Burkhard, and D. K. McCarty for providing the samples. B.L. acknowledges financial support from Elf Aquitaine Production (Géochimie Minérale laboratory in Pau, France), and technical support from the U.S.G.S. in Denver, where this study was done. B.L. thanks D. D. Eberl and B. Velde for fruitful discussions. This paper greatly benefited from constructive comments of Editor R. E. Ferrell, of Associate Editor D. L. Bish and of two anonymous reviewers.

<sup>1</sup> *Laboratoire de Géologie  
Ecole Normale Supérieure  
24 rue Lhomond  
75231 Paris Cedex 05, France*

<sup>2</sup> *Institut de Géologie  
11 rue Emile Argand  
CH 2007 Neuchâtel, Switzerland*

BRUNO LANSON<sup>1\*</sup>  
BERNARD KUBLER<sup>2</sup>

## REFERENCES

- Baggerly, R. G. (1974) X-ray analysis of Ti<sub>3</sub>Al precipitation in Ti-Al alloys: *Adv. X-ray Anal.* **18**, 502–513.
- Bertaut, F. (1950) Raies de Debye-Scherrer et répartition des dimensions des domaines de Bragg dans les poudres polycristallines: *Acta Crystallog.* **3**, 14–18.
- Bienenstock, A. (1961) Determination of crystallite size distributions from X-ray line broadening: *J. Appl. Phys.* **32**, 187–189.
- Brindley, G. W. (1980) Order-disorder in clay mineral structures: in *Crystal Structures of Clay Minerals and Their X-ray Identification*, G. W. Brindley and G. Brown, eds., Mineral Soc., London **2**, 125–195.
- Burkhard, M., Kerrich, R., Maas, R., and Fyfe, W. S. (1992) Stable and Sr-isotope evidence for fluid advection during thrusting of the Glarus nappe (Swiss Alps): *Contrib. Mineral. Petrol.* **12**, 293–311.
- Delhez, R., Keisler, T. H. de, and Mittemeijer, E. J. (1982) Determination of crystallite size and lattice distortions through X-ray diffraction line profile analysis: Recipes, methods, and comments: *Fresenius Z. Anal. Chem.* **312**, 1–16.
- Eberl, D. D. and Blum, A. (1993) Illite crystallite thickness by X-ray diffraction: in *CMS Workshop Lectures, Vol. 5, Computer Applications to X-ray Powder Diffraction Analysis of Clay Minerals*, R. C. Reynolds and J. R. Walker, eds., Clay Minerals Society, Boulder, 124–153.
- Eberl, D. D. and Srodon, J. (1988) Ostwald ripening and interparticle-diffraction effects for illite crystals: *Amer. Mineral.* **73**, 1335–1345.
- Eberl, D. D., Srodon, J., Kralik, M., Taylor, B. E., and PETERMAN, Z. E. (1990) Ostwald ripening of clays and metamorphic minerals: *Science* **248**, 474–477.
- Eberl, D. D. and Velde, B. (1989) Beyond the Kubler index: *Clay Miner.* **24**, 571–577.
- Huang, T. C. and Parrish, W. (1978) Characterization of thin films by X-ray fluorescence and diffraction analysis: *Adv. X-ray Anal.* **22**, 43–63.
- Keijsers, T. H. de, Langford, J. I., Mittemeijer, E. J., and Vogels, A. B. P. (1982) Use of the Voigt function in a single-line method for the analysis of X-ray diffraction line broadening: *J. Appl. Cryst.* **15**, 308–314.
- Klug, H. P. and Alexander, L. E. (1974) *X-ray Diffraction Procedures for Polycrystalline and Amorphous Materials*, Wiley, New York, 966 pp.
- Kodama, H., Gatineau, L., and Méring, J. (1971) An analysis of X-ray diffraction line profiles of microcrystalline muscovites: *Clays & Clay Minerals*, **19**, 405–413.
- Lanson, B. and Besson, G. (1992) Characterization of the end of smectite-to-illite transformation: Decomposition of X-ray patterns: *Clays & Clay Minerals* **40**, 40–52.
- Lanson, B. and Champion, D. (1991) The I/S-to-illite reaction in the late stage diagenesis: *Amer. J. Sci.* **291**, 473–506.
- Lanson, B. and Velde, B. (1992) Decomposition of X-ray diffraction patterns: A convenient way to describe complex diagenetic smectite-to-illite evolution: *Clays & Clay Minerals* **40**, 629–643.
- Louër, D. (1986) Analysis of the broadening of powder diffraction peaks for ZnO: A test case: *Chemica Scripta* **26A**, 17–22.
- Louër, D. and Langford, J. I. (1988) Peak shape and resolution in conventional diffractometry with monochromatic X-rays: *J. Appl. Cryst.* **21**, 430–437.
- Righi, D. and Meunier, A. (1991) Characterization and genetic interpretation of clays in an acid brown soil (dystrochrept) developed in a granitic saprolite: *Clays & Clay Minerals* **39**, 519–530.
- Roof, R. B. Jr. (1971) The effect of self-irradiation on the lattice of <sup>238(80%)PuO<sub>2</sub></sup>: *Adv. X-ray Anal.* **15**, 307–318.
- Sato, T., Watanabe, T., and Otsuka, R. (1992) Effects of layer charge, charge location, and energy change on expansion properties of dioctahedral smectites: *Clays & Clay Minerals* **40**, 103–113.
- Siemens (1990) *Diffra 5000 powder diffraction evaluation software reference manual: Release 2.2*, Siemens Analytical Instruments Inc., Madison, Wisconsin.
- Srodon, J. (1980) Precise identification of illite/smectite interstratifications by X-ray powder diffraction: *Clays & Clay Minerals* **28**, 401–411.
- Velde, B., Suzuki, T., and Nicot, E. (1986) Pressure-temperature-composition of illite/smectite mixed-layer minerals: Niger delta mudstones and other examples: *Clays & Clay Minerals* **34**, 435–441.
- Wagner, C. N. J. and Aqua, E. N. (1963) Analysis of the broadening of powder pattern peaks from cold-worked face-centered and body centered cubic metals: *Adv. X-ray Anal.* **7**, 46–65.
- Warren, B. E. and Averbach, B. L. (1950) The effect of cold-work distortion on X-ray patterns: *J. Appl. Phys.* **21**, 595–599.
- Warren, B. E. and Averbach, B. L. (1952) The separation of cold-work distortion and particle size broadening in X-ray patterns: *J. Appl. Phys.* **23**, 497.

(Received 12 March 1993; accepted 28 March 1994; Ms. 2347)

\* Present address: EAP CSTJF, Laboratoire de géochimie minérale, 64018 Pau Cedex, France.